

# CONCEPTUAL DESIGN OF SC LINAC FOR RIBF-UPGRADE PLAN

K. Yamada\*, K. Suda, N. Sakamoto, and O. Kamigaito,  
RIKEN Nishina Center, Wako, Saitama 351-0198, Japan

## Abstract

An upgrade plan for the RIKEN RI-Beam Factory is under discussion, the objective being to significantly increase the uranium beam intensity. The upgrade will change the first half of the accelerator chain of the RIBF almost completely. For example, the first ring cyclotron will be replaced by a new linac, mainly consisting of superconducting (SC) cavities, which will boost the uranium beam from the RILAC2 injector to 11 MeV/u. The present status of the design study of the new linac is summarized in this paper. The choice of the modular structure, basic specification parameters, and initial design of the SC cavity will be discussed.

## INTRODUCTION

The Radioactive Isotope Beam Factory (RIBF) [1] at the RIKEN Nishina Center was established in order to produce the world's most intense radioactive isotope (RI) beams over the entire range of atomic masses. Among various heavy-ion beams, the uranium beam is one of the most important beams in RIBF, because the in-flight fission of uranium ions can produce intense neutron-rich RI beams far from the stability line on the nuclear chart. The maximum intensity of the uranium beam has recently reached 15 pA ( $\approx 10^{11}$  pps) at 345 MeV/u, owing to the continuous efforts in the past [2]. The intensity of the uranium beam is to be increased at least by a factor of three in the next few years.

Recently, an upgrade plan for RIBF has been proposed with the objective of expanding its capabilities to the study of nuclear reaction mechanisms with RI beams. The beam intensity mentioned above is, however, insufficient to meet this demand; it should be at least ten times higher than the maximum achievable intensity with the present RIBF accelerators. The difficulty in the present acceleration scheme shown in the upper half of Fig. 1 mainly stems from the two-stage charge stripping located at 11 and 50 MeV/u, respectively, which yields a total stripping efficiency of 5% at most. In addition, the RF frequency of the RILAC2 injector [3], 36.5 MHz, is twice that of the succeeding ring cyclotron (RRC), which causes beam losses in the RRC despite the use of the prebuncher operating at 18.25 MHz.

Therefore, we proposed the new acceleration scheme shown in the lower half of Fig. 1. First, the fRC will be replaced by a new cyclotron (New fRC) that will be designed to accept the  $U^{35+}$  ions without charge stripping; the required K-value and RF frequency will be 2,300 MeV and 36.5 MHz, respectively. Second, a new linac, mainly consisting of superconducting (SC) cavities, will replace

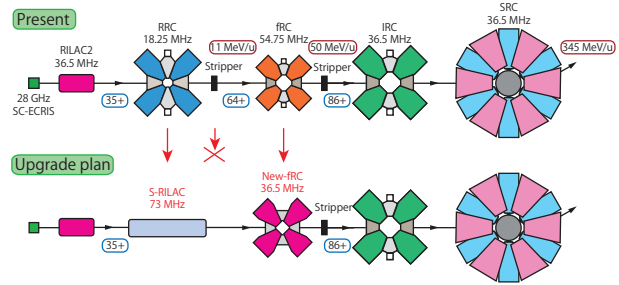


Figure 1: Present (upper half) and proposed (lower half) accelerator chains for the uranium beam at RIBF. The final beam energy is 345 MeV/u. The RF frequencies, stripping energies, and charge states are indicated.

the RRC. The RF frequency is chosen to be 73 MHz, as mentioned below, and the beam transmission is expected to be improved. This linac is also free from the potential risk of space charge effects expected in the RRC at higher beam currents in the future. By these modifications, we aim to increase the beam intensity by at least one order of magnitude compared to the achievable beam intensity with the present accelerator chain.

In order to evaluate the feasibility, we started a design study of the SC linac recently. This paper summarizes the present status of the study.

## OVERVIEW OF NEW LINAC

The new linac is designed to accelerate heavy ions with a mass-to-charge ratio ( $m/q$ ) of  $\sim 7$ , such as  $^{238}U^{35+}$  and  $^{124}Xe^{19+}$ , up to an energy of 11 MeV/u in the cw mode. A layout plan of the new linac is shown in Fig. 2. The present injector, RILAC2, will be used for the low-energy end. We will add a short room-temperature (RT) section to RILAC2, which will boost the beam energy from 0.68 to 1.4 MeV/u. The main part is the succeeding superconducting (SC) section working in the energy range from 1.4 to 11 MeV/u.

The beam energy at the border of the RT and SC sections

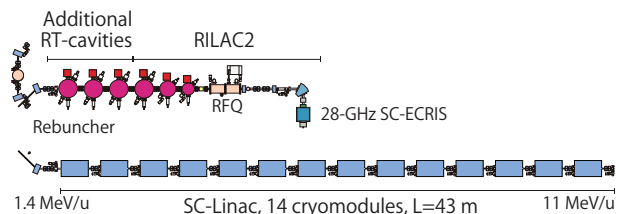


Figure 2: Layout plan of new linac injector.

\*nari-yamada@riken.jp

was chosen so that the SC section could be covered by a single structure of a quarter-wavelength resonator (QWR). As shown below, a sufficiently high acceleration efficiency was obtained by optimizing the dimensions of the SC-QWR. On the other hand, the RT section requires three additional resonators operated at 36.5 MHz that follow the RILAC2 injector directly. The designed gap voltages of the three resonators are 260, 320, and 320 kV, respectively, for the gap numbers 8, 6, and 6, respectively. We also roughly designed the resonators based on the QWR structure in the same manner as the DTL resonators of RILAC2 [4]. The inner diameters of the three resonators could be made common (1300 mm), and each resonator could be excited by an RF amplifier with a maximum output power of 40 kW.

The SC section consists of 14 cryomodules, each of which contains four QWRs operated at 73 MHz. A quadrupole doublet is placed in each gap between the cryomodules. The total length will be 43 m for the SC section. The design procedure is presented below.

## DESIGN STUDY OF SC SECTION

We first chose the RF frequency to be 73 MHz, which is twice that of the RILAC2. It should be noted that the QWRs of the intensity upgrade program of ATLAS at ANL operate at a similar frequency in the similar velocity region [5]. The gap voltage was assumed to be 800 kV.

Second, the gap length and cavity diameter were optimized so as to minimize the number of QWRs involved in the section. The energy gain of each gap was calculated based on the hard-edge approximation. The RF phases at the centers of the two gaps in a QWR,  $\phi_{\text{gap1}}$  and  $\phi_{\text{gap2}}$ , were assumed to have the following relations with the length between the gap centers  $d$ :

$$\phi_{\text{gap1}} = \frac{\pi}{2} + \phi_s - \frac{\pi d}{\beta_0 \lambda}, \quad (1)$$

$$\phi_{\text{gap2}} = \phi_{\text{gap1}} + \frac{2\pi d}{\beta_1 \lambda} - \pi, \quad (2)$$

where  $\beta_0$  and  $\beta_1$  are the injection velocities to the first and second gaps, respectively, and  $\phi_s$  is the synchronous phase, which was chosen to be  $-25^\circ$ . After several iterations, we have determined that  $d = 160$  mm with a total cavity number of 56. The gap length was decided to be 60 mm. The value of  $d$  corresponds to  $\beta_{\text{geom}} = 0.078$  through the relation  $d = \beta_{\text{geom}} \lambda / 2$ . The evolution of the transit time factor for each QWR is plotted in Fig. 3.

The modular configuration of the SC section was optimized based on the first-order approximation for the transverse and longitudinal motions in the next step. The following four configurations were checked for whether a semi-periodic envelope could be obtained or not with moderate-strength focusing elements, while keeping the longitudinal acceptance large enough to capture the output beam from the RT section:

- 5 QWRs + SC solenoid in one cryomodule; 11 cryomodules in total.

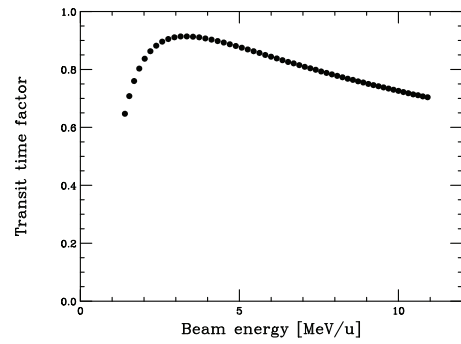


Figure 3: Transit time factor of the designed QWR plotted as a function of beam energy from 1.4 to 11 MeV/u. Fifty-six QWRs are involved.

- 3 QWRs + SC solenoid + 2 QWRs in one cryomodule; 11 cryomodules in total.
- 4 QWRs in one cryomodule + RT quadrupole doublet in between; 14 cryomodules in total.
- 3 QWRs in one cryomodule + RT quadrupole doublet in between; 18 cryomodules in total.

The spatial separation between the cavities was fixed to be 400 mm in all cases. Realistic spaces were kept between the other components for mounting necessary instruments such as valves and diagnostics boxes.

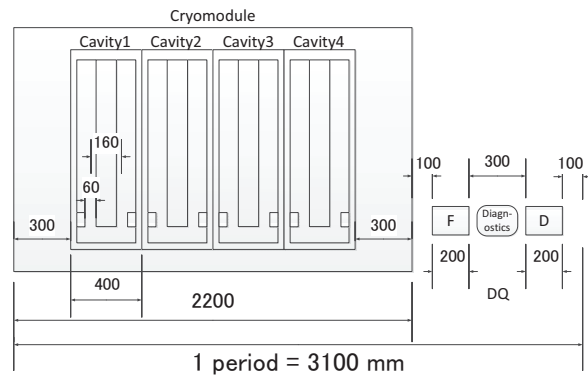


Figure 4: Selected layout plan of one periodic structure.

It was found that the first case listed above had an insufficient longitudinal acceptance, while the second case had a large acceptance. However, we chose the configuration shown in Fig. 4 for the SC section; the third case listed above. This configuration did not give the best longitudinal acceptance among the four. However, the advantage is that the RT quadrupoles, having an aperture diameter of 50 mm and a field gradient of less than 20 T/m, would be easier to make and operate compared to the SC solenoid. The separation between the quadrupole magnets was set as 0.3 m for mounting the diagnostics box.

The transverse and longitudinal beam envelopes are also plotted by using the TRACE3-D code [6] in Fig. 5. The ini-

tial longitudinal ellipse was assumed to have a phase spread of  $\Delta\phi = \pm 10^\circ$  and an energy spread of  $\Delta E/E = \pm 3.0\%$ ; these values were larger than the calculated longitudinal emittance of the output beam from the RT section. As shown in Fig. 5, the envelopes are kept small enough.

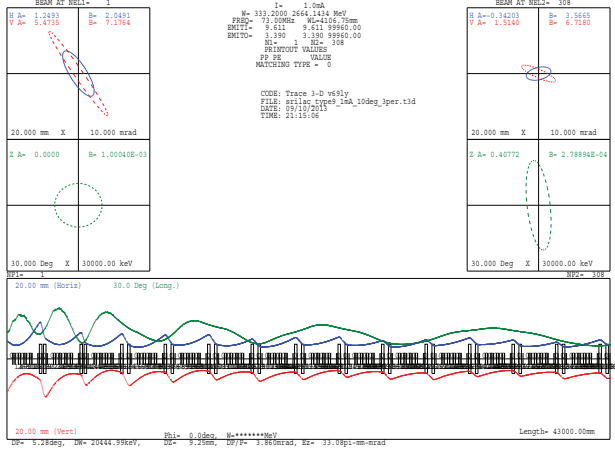


Figure 5: Transverse and longitudinal beam envelopes plotted by TRACE3-D code.

The initial designs of the SC QWR were carried out using CST Microwave Studio 2013 (MWS). Figure 6 shows the magnetic-field distribution in the QWR. The SC cavity will be operated at 4.5 K. The RF surface resistance is assumed to be 25 nΩ on the safe side, where the BCS resistance is negligibly small. The parameters of the SC section at present are listed in Table 1. Here, the definition of  $E_{acc}$  is selected to be the inner diameter of the cavity.

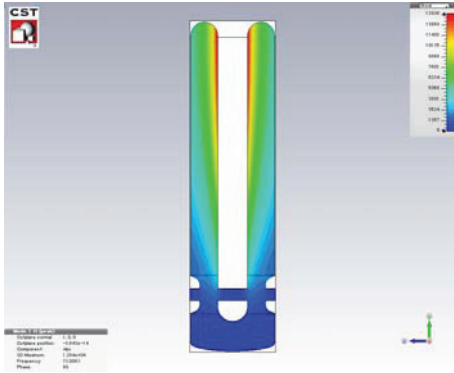


Figure 6: Magnetic-field strength of the QWR calculated by MWS.

## OUTLOOK

Although the conceptual design of the new linac is still at the initial stage, we have obtained a reasonable solution to meet the requirement. Further study is under way on the SC QWR, including the mechanical considerations, tuner design, and coupler design. In parallel, we are going to

**02 Future projects**

**C. Future Project**

Table 1: Design parameters of the SC section of the new linac.

Frequency [MHz]	73
Duty [%]	100
Mass-to-charge ratio (m/q)	~7
Input energy [MeV/u]	1.4
Output energy [MeV/u]	11.0
Number of cavities	56
Number of cryomodules	14
Number of quadrupole magnets	28
Total length [m]	43
<hr/>	
Cavity inner diameter [mm]	φ280
Cavity height [mm]	1103
Gap length $g$ [mm]	60
Gap voltage $V_{gap}$ [kV]	800
$\beta_{geom}$ of cavity	0.078
Beam aperture $a$ [mm]	φ40
Synchronous phase $\phi_s$ for $\beta_{geom}$ [°]	-25
Operating temperature $T$ [K]	4.5
$G = Q_0 \times R_s$ [Ω]	21.0
$R_a/Q_0$ [Ω]	601.9
$R_s = R_{BCS} + R_{res}$ [nΩ]	25
$Q_0$	$8.4 \times 10^8$
Shunt impedance $R_a$ [Ω]	$5.1 \times 10^{11}$
Rf power loss $P$ [W]	5.1
$E_{acc}$ [MV/m]	5.1
$E_{peak}/E_{acc}$	6.1
$B_{peak}/E_{acc}$ [mT/(MV/m)]	11.6

start thermal and mechanical studies of cryostats based on the initial design shown above. We expect to complete the first mechanical drawing of the cryomodule by the end of this year.

## REFERENCES

- [1] Y. Yano, Nucl. Instr. Meth. B **261**, 1009 (2007).
- [2] H. Okuno, N. Fukunishi, O. Kamigaito, Prog. Theor. Exp. Phys. (2012) 03C002. N. Fukunishi et al., CYCLOTRONS'13, Vancouver (2013).
- [3] K. Yamada et al., Proc. of IPAC'12, TUOBA02, 1071 (2012).
- [4] K. Suda et al., Nucl. Instr. Meth. A **722**, 55 (2013).
- [5] P.N. Ostroumov et al., Proc. of LINAC'12, TUPLB08, 461 (2012).
- [6] [http://laacg.lanl.gov/laacg/services/download\\_trace.phtml](http://laacg.lanl.gov/laacg/services/download_trace.phtml).